Modelling of Iron Flow, Heat Transfer, and Refractory Wear in the Hearth of an Iron Blast Furnace

P K Iwamasa[1], G A Caffery[1], W D Warnica[2], S R Alias[3]

1. BHP Research - Newcastle Laboratories, Shortland, NSW, Australia
2. Hatch Associates Ltd., Mississauga, Ontario, Canada
3. Advanced Scientific Computing Ltd., Waterloo, Ontario, Canada

ABSTRACT

There is a world wide initiative to extend blast furnace campaigns to defer capital expenditures and reduce production costs. Most efforts to accomplish this goal at BHP Steel are focussed on the hearth. The wear of hearth refractory has the greatest influence over the life of the furnace. One aspect of this asset life extension program is the development of a model for computing hearth conditions of typical blast furnace operations. This CFD application is complicated by its wide range of geometric scales (60 mm taphole and 10 m hearth), porous flow, thermal stratification, solidification, and conjugate heat transfer.

Commercial software TASCflow™ has been used to compute iron flow and temperature fields. Refractory wear was predicted based on laboratory measurements. This hearth model has been used to simulate blast furnace operations and to estimate the effects of changing conditions on hearth wear. It has proved to be a useful tool to develop operational strategies which control wear.

NOMENCLATURE

C_m Morphology constant
d Coke diameter
h Heat transfer coefficient
k_e Effective mass transfer parameter
q Heat flux
T Temperature
T_L Temperature - liquidus
T_S Temperature - solidus
V Local interstitial fluid velocity
δ Small constant - for stability
ε Porosity
μ Viscosity
ρ Density
τ Shear stress at iron - refractory interface in blast furnace hearth
τ_O Reference shear stress based on the rotating disc experiment

1. INTRODUCTION

There is a growing world wide initiative to extend the life of an iron blast furnace to campaigns of 15 to 20 years. The condition of the hearth refractory is the limiting factor in the life of a blast furnace so operating the furnace to control and minimise refractory wear results in a direct benefit in an extended campaign. This project was initiated to investigate how blast furnace operations influence refractory wear using a three dimensional computational model of the iron blast furnace.

A commercial computational fluid dynamic (CFD) package, TASCflow, was used to solve for iron flow and heat transfer and to predict refractory wear in the hearth of a blast furnace. TASCflow uses a hybrid finite volume and finite element method which solves the three dimensional Reynolds averaged Navier-Stokes equation for fluid flow within complex geometries.

The blast furnace hearth used in this study was the Flat Products Division Port Kembla Steelworks Blast Furnace 6 (PK6).

2. MODEL DESCRIPTION

This work is an extension of initial studies completed at BHP Research[1] and Advanced Scientific Computing[2] where an idealised hearth geometry was used.

2.1 Iron Blast Furnace

A schematic of an iron blast furnace is shown in Figure 1. Iron oxide, coke, and fluxes are

charged into the top of the shaft. A blast of heated air and other fuels are introduced through the blow pipes. The heated air burns the injected fuels and coke which provide the energy and reducing gases to transform the iron oxides to liquid iron. This iron is collected in the hearth and is removed from the furnace via the taphole. The unburnt coke makes its way to the hearth and forms a "deadman". The deadman provides the strength to support the burden of the furnace.

2.2 Hearth Geometry

The dimensions (in mm) of the blast furnace hearth geometry cross-section are presented in Figure 2. The complexity of modelling the blast furnace is inherent in the variation of scales within the hearth. Adequate resolution of the grid is included in the small (60 mm diameter) taphole as well as the large (10 m diameter) hearth proper and therefore the computational domain is quite large.

2.2.1 Refractory Regions

The computational grid of the refractory regions generated using ICEM CFD Powermesh is shown in Figure 3. This figure shows the regions in which only heat transfer was modelled as it did not contain fluid.

2.2.2 Iron and Coke Regions

The hearth refractory contains the molten iron and the coke deadman. The iron is removed from the blast furnace through a taphole. The entire computational domain consisting of 113,566 active nodes is shown in Figure 4.

2.3 Boundary Conditions

The boundary conditions of the problem were defined with the following properties:

Top Refractory Walls:
The refractory walls at the top of the hearth (where the hearth is attached to the rest of the blast furnace) were set to be adiabatic.

Refractory Bottom Wall:
The bottom of the furnace is set at a constant temperature of 50° C.

Shell Wall:
A heat transfer coefficient (h = 180 W m^{-2} K^{-1})[3] and a far field temperature was used to specify a heat flux at the shell of the furnace (T_O = 25 °C). The heat flux is defined by the following equation.

$$q = h\,(T - T_O) \qquad (1)$$

Fluid Walls:
All refractory walls adjacent to the iron are modelled as hydrodynamically smooth with the code ensuring a continuity of temperature across the interface.

Symmetry Wall:
A symmetry wall was used through the vertical cross section of the hearth through the centre of the taphole.

Opening Boundary:
The top of the hearth was set as an opening boundary where the total pressure (10^5 Pa) and inlet temperature were specified.

Outflow Boundary:
The mass flowrate of molten iron was set at the outlet of the taphole.

2.4 Physical Models

Because of the complex nature of the flow in the hearth of the blast furnace, five physical models were incorporated into the fluid flow package. These models include fluid turbulence, conjugate heat transfer, porous media losses, solidification of iron in the hearth, and wear of the refractory.

2.4.1 Fluid Turbulence

The standard two equation k-ε turbulence model was used for this application.

2.4.2 Heat Transfer

The coupled heat transfer between the refractory and iron regions of the hearth was modelled using TASCflow's Conjugate Heat Transfer (CHT) module. As a result of the imposed cooling of the hearth, temperature gradients exists within the furnace inducing buoyancy driven flow. Natural convection is modelled using a Boussinesq formulation.

2.4.3 Porous Media Losses

The coke in the hearth is modelled as a packed bed with a coke diameter of 30 mm which provides a resistance to flow resulting in momentum losses. The porous media losses

were modelled using Ergun's equation which describes pressure losses in terms of kinetic and viscous energy losses.[4]

$$\vec{\nabla}P = -(\alpha V + \beta V^2) \qquad (2)$$

where

$$\alpha = \frac{150\mu(1-\varepsilon)}{(\varepsilon d)^2} \qquad (3)$$

$$\beta = \frac{1.75\rho(1-\varepsilon)}{\varepsilon d} \qquad (4)$$

2.4.4 Iron Solidification

When the operating conditions of the furnace cause the interface between the iron and the refractory to fall below the liquidus temperature, solidification of iron on the refractory occurs. Solidification of iron was modelled in a manner similar to that of porosity where a source term for the resistance to flow is proportional to the amount of iron that solidifies in the control volume. The local liquid fraction is defined in terms of the local, solidus, and liquidus temperatures as shown in Table 1.

Table 1: Volume fraction of liquid as a function of local temperature

Temperature	Liquid Fraction (F_{liq})
$T < T_S$	0
$T_S \le T \le T_L$	$\frac{T - T_S}{T_L - T_S}$
$T > T_L$	1

The resulting momentum loss that was incorporated in the code is:

$$\vec{\nabla}P = -\sigma\vec{V} \qquad (5)$$

where

$$\sigma = C_m \frac{(1-F_{liq})^2}{F_{liq}^3 + \delta} \qquad (6)$$

2.4.5 Refractory Wear

Refractory wear rate coefficients were calculated in the post-processing stage of the simulation. The equations used in the refractory wear model were based on work carried out at BHP Research where a rotating disc apparatus was used to wear test the carbon brick refractory BC7S.[5] Based on the rotating disc theory, the following equation for wear rate coefficient, $\dot{w}$, was implemented into the model.

$$\dot{w} = k_e \left(\frac{\tau}{\tau_O}\right)^{1/3} \qquad (7)$$

The effective mass transfer parameter, k_e, is a measure of the rate of dissolution of the refractory.

$$k_e = \frac{1}{100} \exp\left[2.8956 - \left(\frac{11344}{T}\right)\right] \qquad (8)$$

3. PROCESS DESCRIPTION

3.1 Operational Conditions

The following operational conditions were used in the comparison of model results.

Production Rate (kg metal s^{-1}):

P_O	80
P_L	70
P_H	90

Coke Bed Porosity:

ε_O	0.30
ε_L	0.15
ε_H	0.45

Deadman Shape:[6,7]

Flat H_O Fully packed heath
H_1 Floating 250 mm
H_2 Floating 500 mm

Angled x_O, ϑ_O, H_O Sitting - Figure 5
x_O, ϑ_O, H_2 Floating - Figure 6

Iron Level (above the top of taphole, mm):

L_O	250
L_L	83
L_H	500

Iron Temperature (at inlet, °C):

T_O	1550
T_L	1475
T_H	1625

3.2 Matrix of Runs

A parametric survey was conducted on the variables described above where each parameter was varied individually. The results were then compared to the base case (Run 1-0).

Table 2: Matrix of runs

ID	P	ε	coke	L	T
1-0	P_O	ε_O	H_O	L_O	T_O
1-1	P_O	ε_O	H_O	L_O	T_L
1-2	P_O	ε_O	H_O	L_O	T_H
1-3	P_O	ε_O	H_O	L_L	T_O
1-4	P_O	ε_O	H_O	L_H	T_O
1-5	P_O	ε_O	H_1	L_O	T_O
1-6	P_O	ε_O	H_2	L_O	T_O
1-7	P_O	ε_O	x_O, ϑ_O, H_O	L_O	T_O
1-8	P_O	ε_O	x_O, ϑ_O, H_2	L_O	T_O
1-9	P_O	ε_L	H_O	L_O	T_O
1-10	P_O	ε_H	H_O	L_O	T_O
1-11	P_L	ε_O	H_O	L_O	T_O
1-12	P_H	ε_O	H_O	L_O	T_O

4. MODEL RESULTS

4.1 Temperature Profiles

The temperature contours in the refractory and iron regions on the symmetry plane for the base case is presented in Figures 7 and 8. A summary plot showing the minimum, maximum, and average temperatures on the interface between the iron and refractory for the entire hearth are shown in Figure 9.

4.2 Streak Lines

The trajectory of particles of zero mass for runs 1-0 and 1-7 are presented in streak plots on the symmetry plane in Figures 10 and 11. In both of these figures, the fluid flows down the wall of the hearth. Buoyancy forces the fluid back up and into a recirculation zone. In Figure 11, the fluid circulates in the area where there is the least resistance to flow, in the coke free regions.

4.3 Fluid Speed

Speed contours of the iron field on the symmetry plane is shown for runs 1-0 and 1-7 in Figures 12 and 13. A zone of acceleration is evident as the fluid approaches the taphole. In Figure 13, the speed of the fluid in the recirculation zone in the coke free region is significant.

4.4 Refractory Wear Coefficient

The refractory wear coefficient [cm s^{-1}] for runs 1-0 and 1-7 is plotted in Figures 14 and 15 at the interface between the iron and refractory. A summary plot showing the minimum, maximum, and average wear rate coefficients are shown in Figure 16.

5. DISCUSSION

5.1 Natural Convection

Heat is extracted from the outer refractory walls by stave cooling and from the hearth bottom by underhearth cooling. The resulting buoyant iron flow is the dominating flow characteristic of these simulations. In all but the run with the low (1475 °C) iron inlet temperature, a recirculation zone forms at the base of the furnace opposite the taphole and extends around the circumference until the influence of forced convection of the taphole causes its collapse.

5.2 Effect of Operational Parameters

5.2.1 Temperature

The temperature of the hot metal entering the hearth influences the ratio of natural convection to forced convection with observed changes in the flow field. When temperature is increased, natural convection is more dominant and therefore increases the recirculation zone and the velocity of the metal at the interface of the iron and refractory. This increased velocity results in a greater amount of refractory wear.

5.2.2 Height of Iron Above Taphole

The influence of the height of iron above the taphole is slight with the greatest effect around the taphole region.

5.2.3 Deadman Porosity and Configuration

The results of this initial study show that the shape and porosity of the coke deadman are the most significant parameters determining the wear of hearth refractory. These factors influence the flow field of the iron which in turn effects the wear rate coefficient.

Porosity

A hearth with a low coke porosity tends to reduce the effect of thermal recirculation and to increase the acceleration zone of iron near the taphole. Therefore, the wear near the taphole is also increased.

Shape and Location of Deadman

The largest single influence of refractory wear is the shape and location of the coke deadman.

A coke free layer allows a high velocity recirculation zone to form on the pad of the hearth, promoting refractory wear. The height and shape of the coke free layer effects the size and shape of the recirculation zone and the maximum velocity within the layer.

5.2.4 Production Rate

As forced convection is less significant compared to natural convection (except for near the taphole), it is expected that changes in production rate will have only a small effect on the flow pattern and hence the wear rate. The influence of production rate may be more significant when considered in conjunction with different parameters such as deadman porosity and configuration.

6. CONCLUSIONS

A three dimensional CFD model for iron flow, heat transfer, and refractory wear in the hearth of a blast furnace was developed. The initial portion of this study consisted of a parametric survey of various operating conditions for PK6. The results obtained in this phase suggest that the shape and location of the coke deadman influences the wear in the hearth refractory the most. Refractory wear is most rapid when the coke is not sitting on the hearth bottom but when it is floating. Perhaps there is a critical height of the coke free layer that causes the greatest amount of wear on the refractory pad.

The results obtained from this initial work are consistent with observed reports of post mortems done on various blast furnaces.[8,9] Figures 15 and 16 show the wear profile of two Kawasaki Steel blast furnaces.[8] The figures show what the model predicts. Greatest refractory wear occurs at the walls and at the bottom of the hearth near the walls. This is caused by the vigorous recirculation zone driven by natural convection. Further verification to the current model with data from thermocouples embedded in the hearth refractories will be conducted.

Future work will include grid refinement to resolve more details in the flow and temperature fields near the hearth walls. Also, underhearth cooling will be included to get a more realistic boundary condition for the bottom of the hearth, and a more accurate description of refractory wear. More work will be carried out to explore the effects of the shape and location of the coke bed on the wear of the refractory. Also, future work will be identified by each of the operating divisions for specific applications.

REFERENCES

[1] Caffery, G., B. E. Honours Thesis, University of Newcastle, November 1995.

[2] Elias, S. R., ASC Report 96-3098-162.

[3] Haywood, R. J., BHP Research Internal Report: BHP/MPR/R/93/016.

[4] Ergun, S., *Chemical Engineering Progress,* Vol. 28, No. 2, pp. 89-94, 1952.

[5] Thomson, A. D., G. A. Caffery, R. I. Olivares, J. Freeman, and W. D. Warnica, *PacRim2, The 2nd International Meeting of Pacific Rim Ceramic Societies*, 15-17 July, 1996, Cairns, Australia.

[6] Shibata, K., Y. Kimura, M. Shimizu, and S. Inaba, *ISIJ International*, Vol. 30, No. 3, 1990, pp. 208-215.

[7] Ohno, J., M. Nakamura, Y. Hara, M. Tachimori, and S. Arino, *International Blast Furnace Hearth and Raceway Symposium*, Newcastle, Australia, 3-6 March, 1981, The Australasian Institute of Mining and Metallurgy, pp. 10:1-12.

[8] Yoshikawa, F. and J. Szekely, *Ironmaking and Steelmaking*, No. 4, 1981, pp.159-168.

[9] Uenaka, T., K. Shimomura, K. Kuwana, K. Uemura, *Ironmaking Proceedings*, Book 2, Vol. 45, 1986, Washington, pp. 185-191.

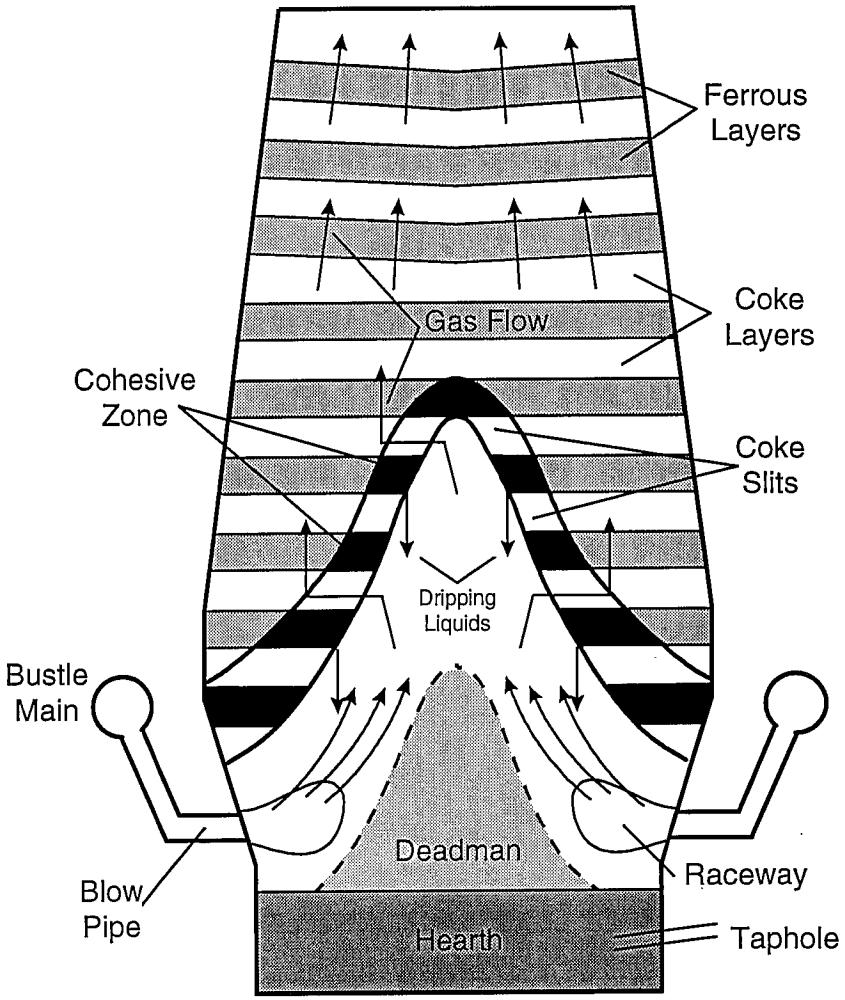

Figure 1: Schematic of an Iron Blast Furnace

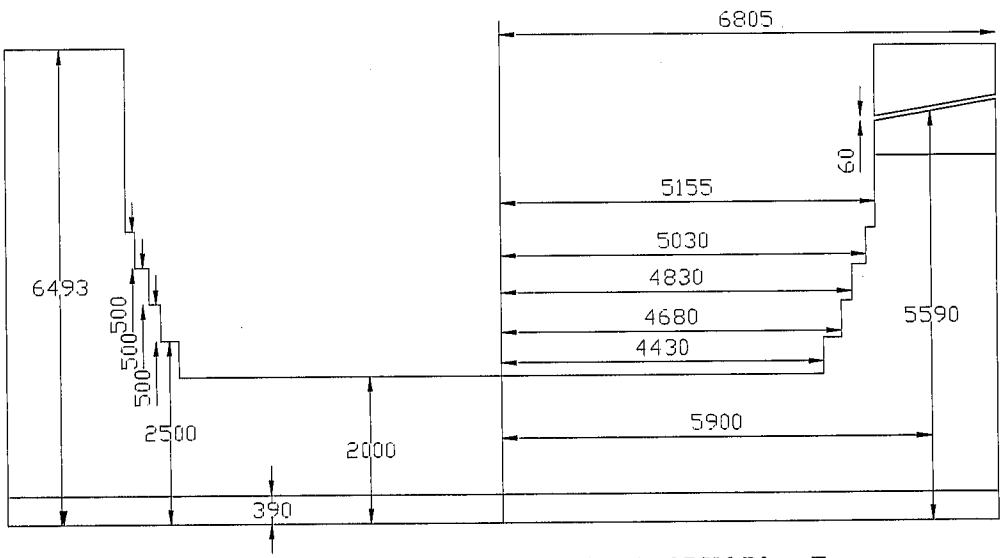

Figure 2: Dimensions (mm) of PK6 Blast Furnace

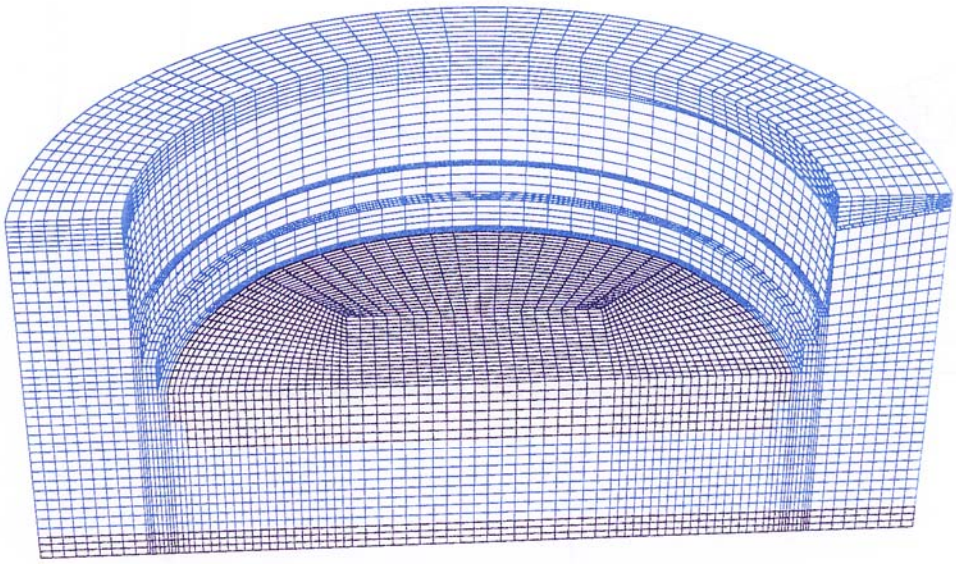

Figure 3: Computational Domain - Refractory

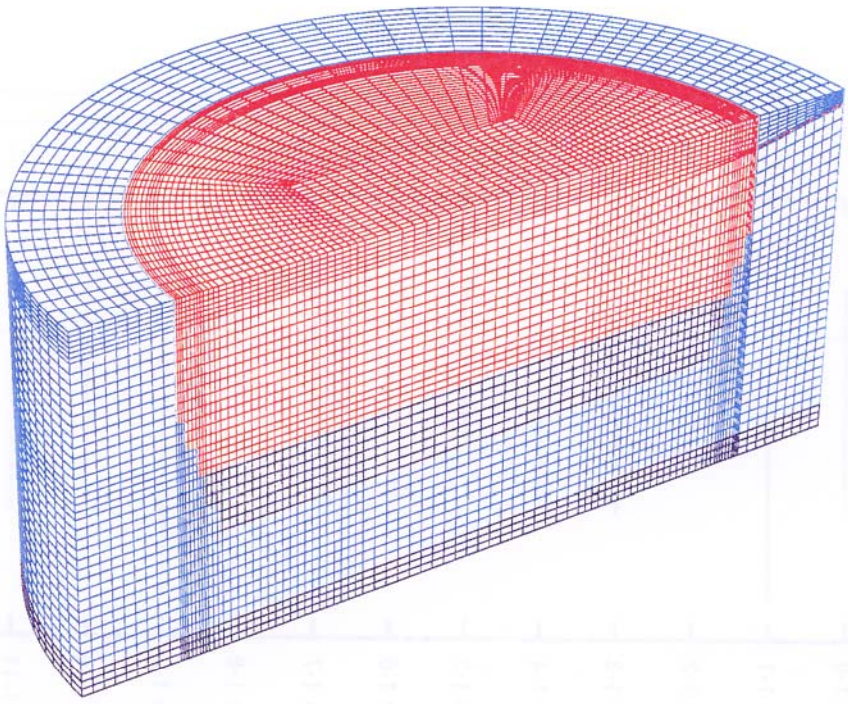

Figure 4: Computational Domain - Refractory and Iron/Coke

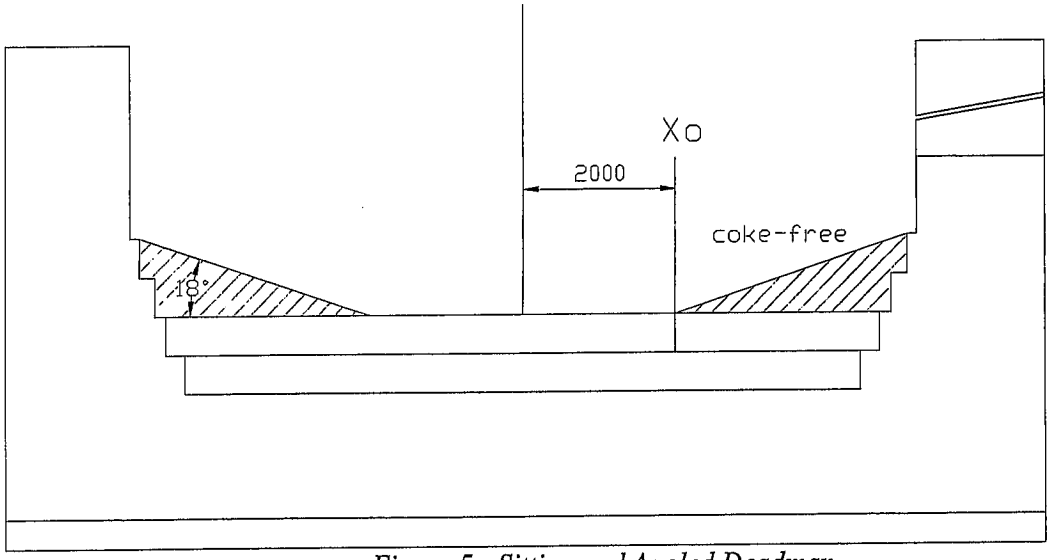

Figure 5: Sitting and Angled Deadman

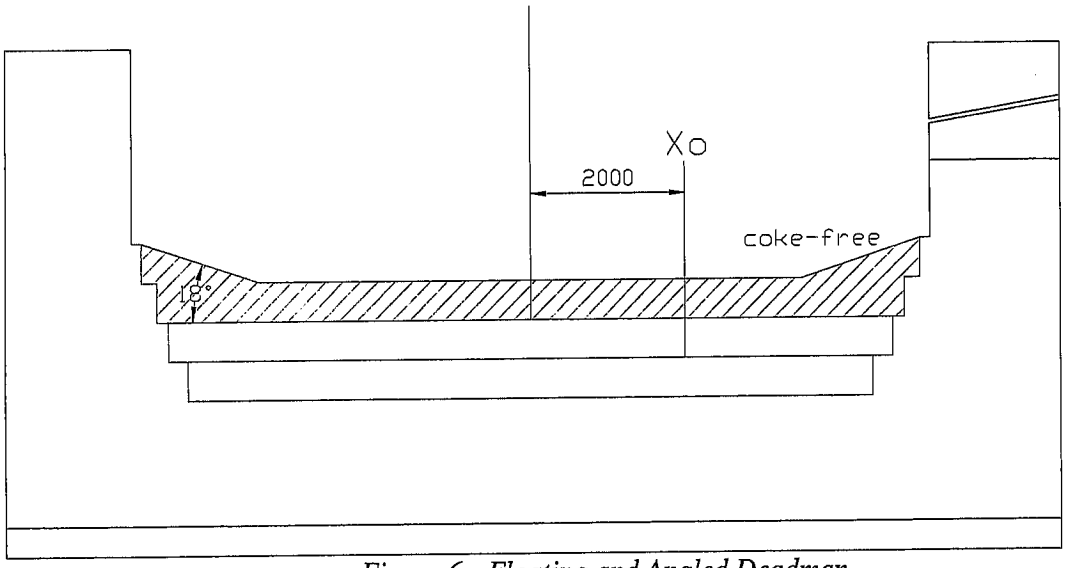

Figure 6: Floating and Angled Deadman

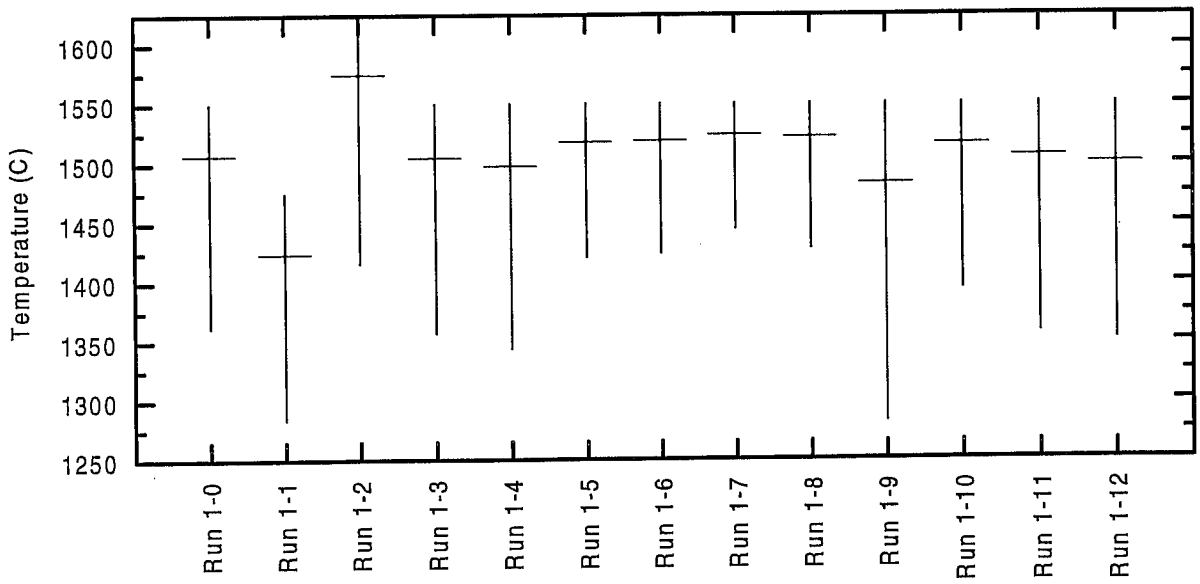

Figure 7: Hearth Refractory Temperatures

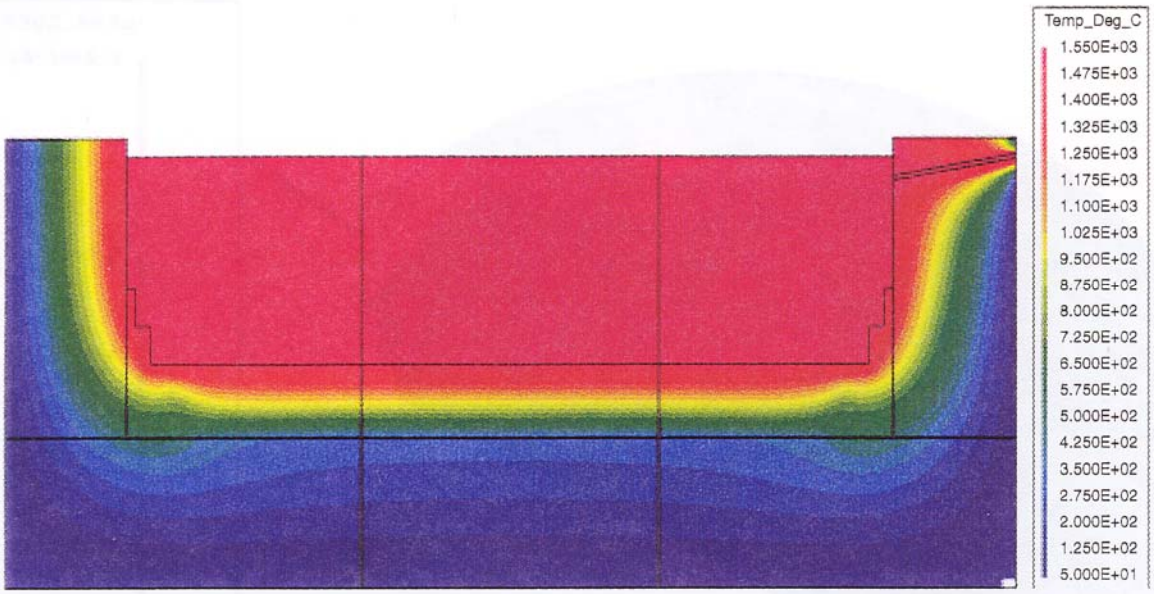

Figure 8: Temperature Profile in the Symmetry Plane, Run 1-0

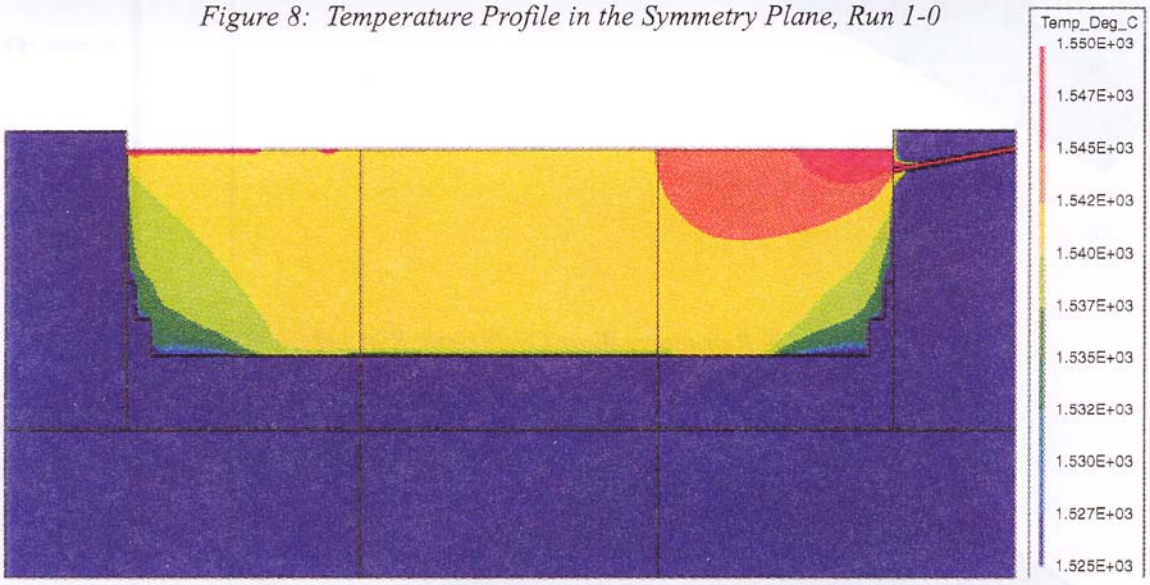

Figure 9: Temperature Profile in the Symmetry Plane, Run 1-0

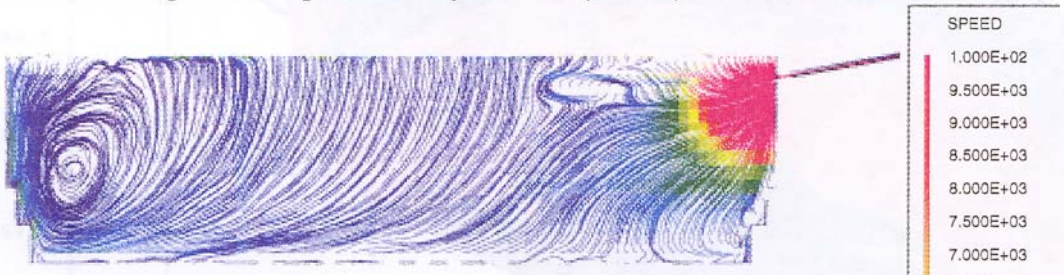

Figure 10: Streak Lines in the Symmetry Plane, Run 1-0

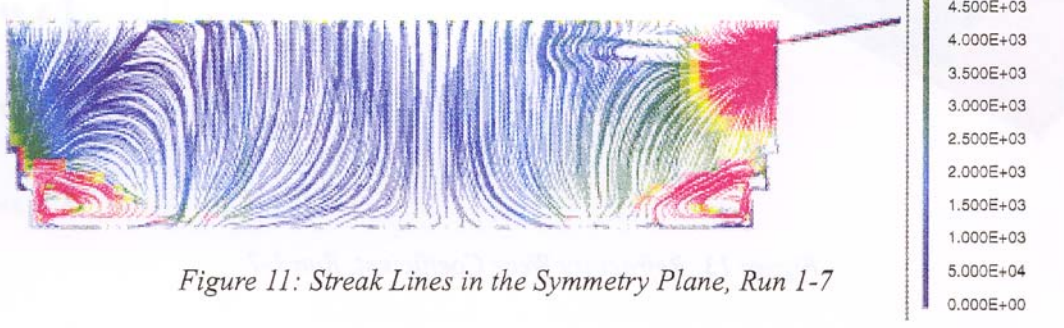

Figure 11: Streak Lines in the Symmetry Plane, Run 1-7

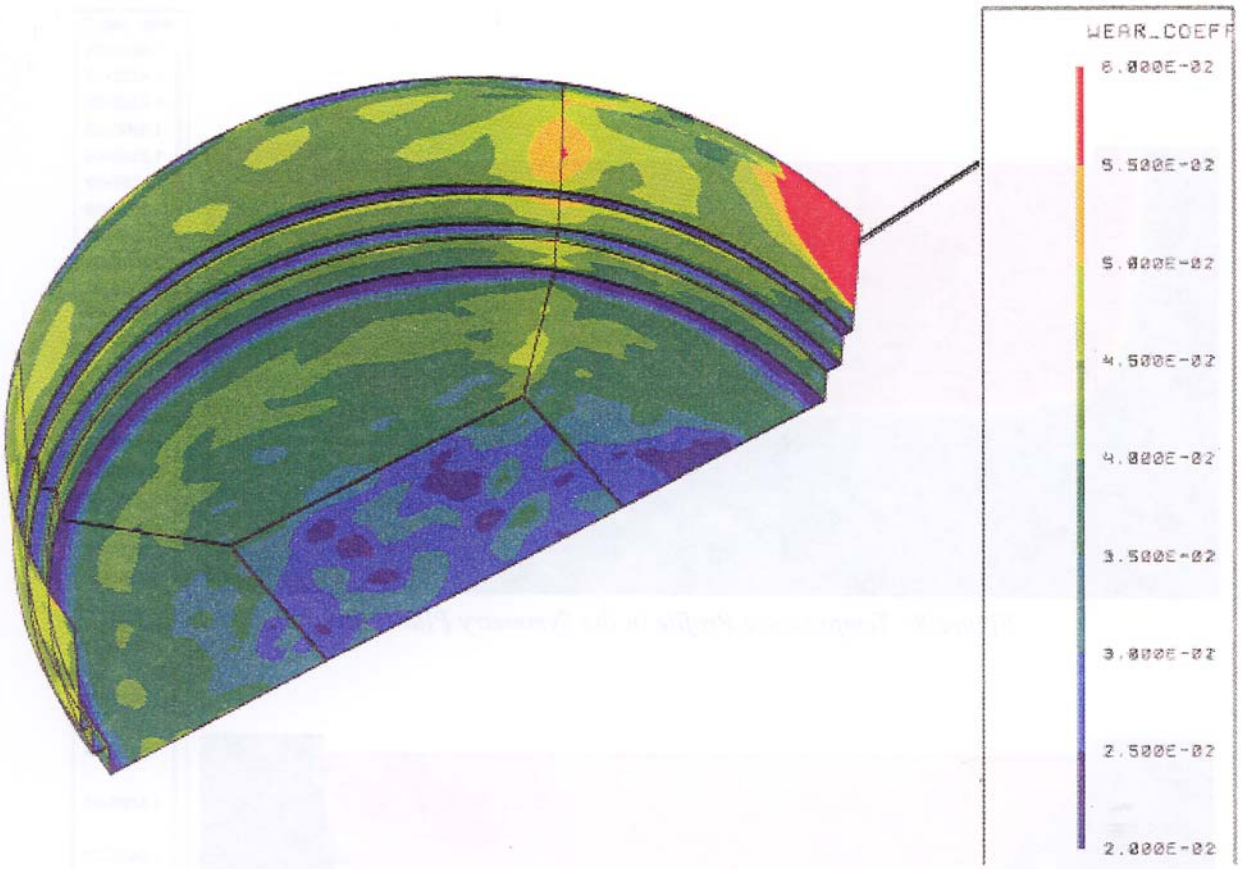

Figure 12: Refractory Wear Coefficient, Run 1-0

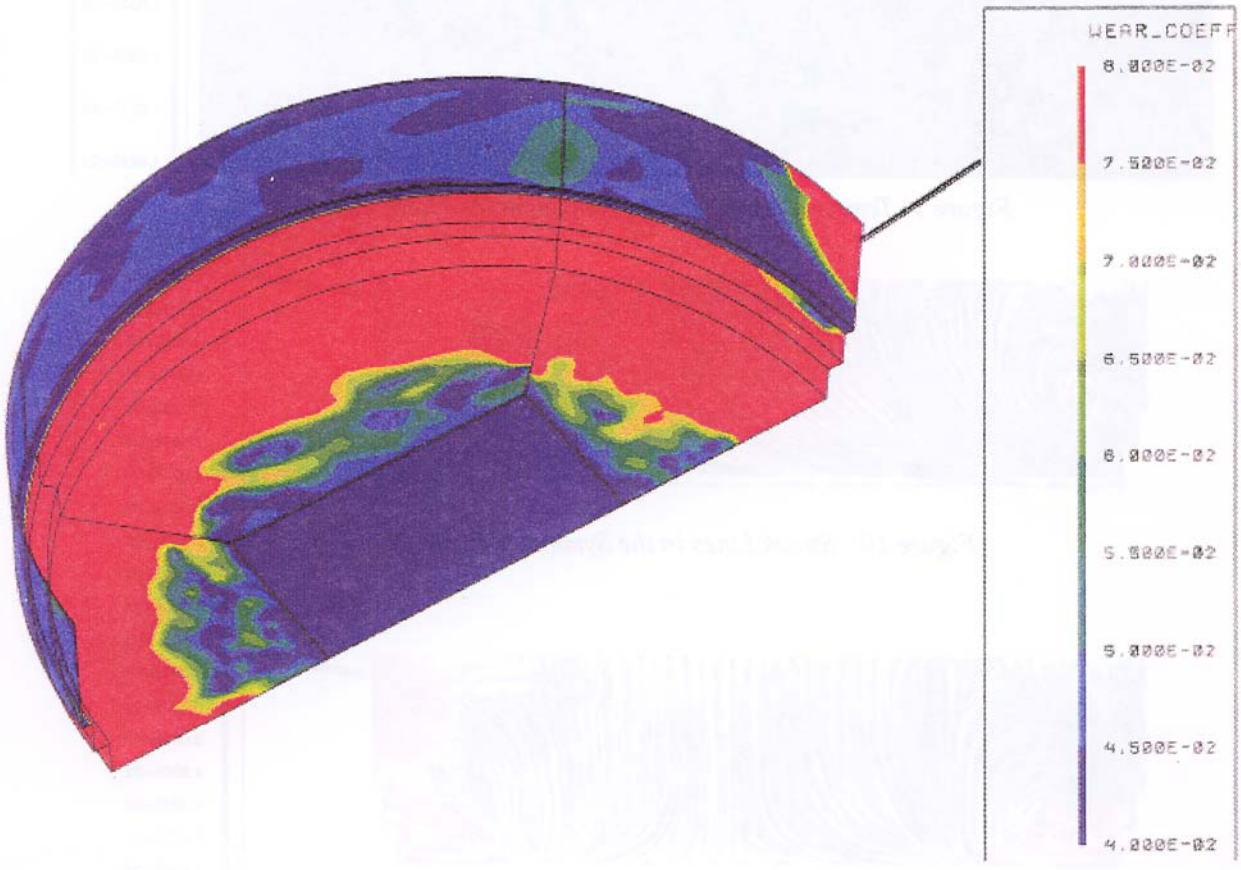

Figure 13: Refractory Wear Coefficient, Run 1-7

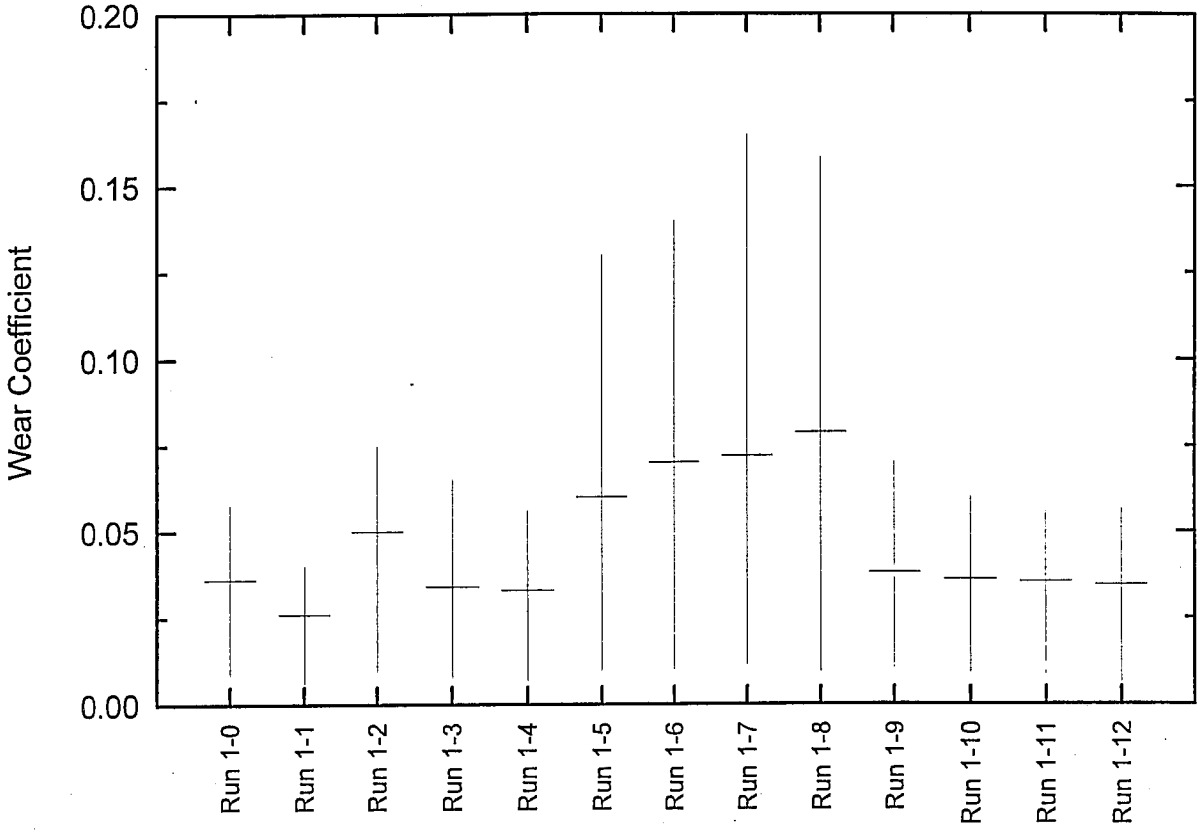

Figure 14: Refractory Wear Coefficient

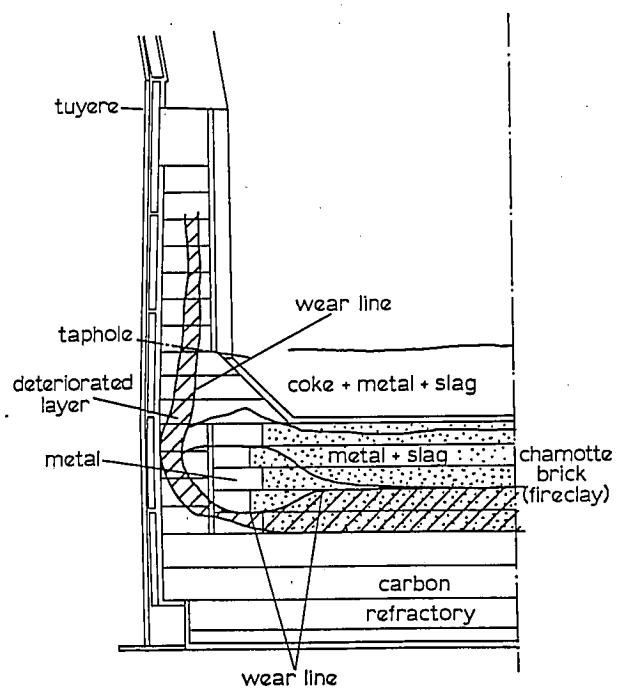

Figure 15: Profile of Wear Line of a Kawasaki Steel Blast Furnace Blown Out After 4.7 Years in Operation[8]

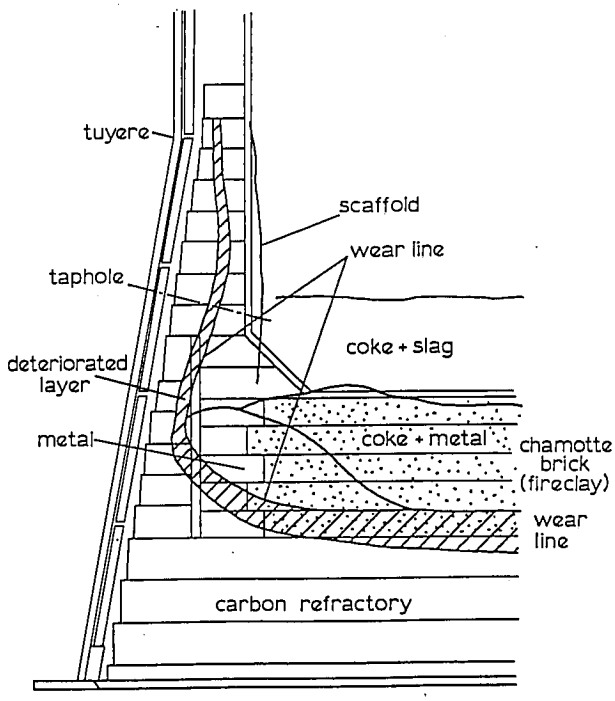

Figure 16: Profile of Wear Line of a Kawasaki Steel Blast Furnace Blown Out After 6.2 Years in Operation[8]